HHS Public Access

Author manuscript

Cell Signal. Author manuscript; available in PMC 2023 March 01.

Published in final edited form as:

Cell Signal. 2022 March ; 91: 110245. doi:10.1016/j.cellsig.2022.110245.

G3bp1 – microRNA-1 axis regulates cardiomyocyte hypertrophy

Saleena Alikunju, PhD[1,*], **Nandita Niranjan, MSc**[1,*], **Maha Mohsin, BSc**[$], **Nazish Sayed, MD, PhD**[#], **Danish Sayed, MD, PhD**[1,†]

[1]Department of Cell Biology and Molecular Medicine, Rutgers New Jersey Medical School, Newark, New Jersey 07103

[#]Cardiovascular Institute, Department of Surgery, Division of Vascular Surgery, Stanford University School of Medicine, Stanford, California 94304

[$]Summer undergraduate student, Rutgers University, New Brunswick, New Jersey

Abstract

Adaptation of gene expression is one of the most fundamental response of cardiomyocytes to hypertrophic stimuli. G3bp1, an RNA binding protein with site-specific endoribonuclease activity regulates the processing of pre-miR-1 stem-loop, and thus levels of cardiomyocyte -enriched mature miR-1. Here, we examine the role of G3bp1 in regulating gene expression in quiescent cardiomyocytes and those undergoing growth-factor induced hypertrophy. Further, we determine if these changes are facilitated through G3bp1-mediated regulation of miR-1 in these cardiomyocytes. Using isolated cardiomyocytes with knockdown of endogenous G3bp1, we performed high throughput RNA sequencing to determine the change in cardiac transcriptome. Then, using gain and loss of function approach for both, G3bp1 and miR-1, alone or in combination we examine the G3bp1-miR-1 signaling in regulating gene expression and Endothelin (ET-1) -induced cardiomyocyte hypertrophy. We show that knockdown of endogenous G3bp1 results in inhibition of genes involved in calcium handling, cardiac muscle contraction, action potential and sarcomeric structure. In addition, there is inhibition of genes that contribute to hypertrophic and dilated cardiomyopathy development. Conversely, an increase is seen in genes that negatively regulate the Hippo signaling, like Rassf1 and Arrdc3, along with inflammatory genes of TGF-β and TNF pathways. Knockdown of G3bp1 restricts ET-1 induced cardiomyocyte hypertrophy. Interestingly, concurrent silencing of G3bp1 and miR-1 rescues the change in gene expression and inhibition of hypertrophy seen with knockdown of G3bp1 alone. Similarly, expression of exogenous G3bp1 reverses the miR-1 induced inhibition of gene expression. Intriguingly, expression of Gfp tagged G3bp1 results in perinuclear accumulations of G3bp1-Gfp,

[†]To whom correspondence should be addressed: Danish Sayed, Department of Cell Biology and Molecular Medicine, Rutgers New Jersey Medical School, 185 South Orange Avenue, Medical Science Building, G-653, Newark, New Jersey 07103, sayeddh@njms.rutgers.edu, Tel. (973) 972-5243.

[*]Contributed equally

Author contributions: SA and NN performed experiments; MM, summer intern assisted is experiments; NS assisted in the conceptual approach and writing; DS designed experiments, performed data analysis with figures and wrote the manuscript.

Declaration of interest: None.

resembling Stress Granules. Based on our results, we conclude that G3bp1 through its regulation of mature miR-1 levels plays a critical role in regulating the expression of essential cardiac-enriched genes and those involved in development of cardiomyocyte hypertrophy.

Keywords

Cardiac hypertrophy; G3bp1; microRNA-1; Stress Granules; Posttranscriptional regulation

1.1 Introduction

RNA binding proteins play critical role in posttranscriptional regulation and hence in modulation of gene expression. Ras GTPase-Activating Protein SH3 Domain-Binding Protein 1 (G3bp1) is an endoribonuclease belonging to heterogenous nuclear RNA binding protein (hnRNP) family [1]. RasGAP dependent phosphorylation of G3bp1 favors site specific endoribonuclease activity [2], [3], while dephosphorylation promotes formation of perinuclear cytoplasmic protein-RNA aggregates called stress granules [4], which function as triage sites for mRNAs [5],[6].

Previously, we reported that G3bp1 posttranscriptionally regulates microRNA-1 (miR-1) biogenesis, where it associates with pre-miR-1 stem-loop and controls miR-1 expression levels in cardiac myocytes [7]. Downregulation of miR-1, seen as early as 24hrs post transaortic constriction (TAC), is required for the accommodation of gene expression and development of cardiac hypertrophy [8], [9]. Several studies have confirmed differential expression of miR-1 during cardiac hypertrophy in mice and cardiomyopathy in humans [8],[10],[11],[12]. These studies suggest that an increase in G3bp1 function might be essential for rapid downregulation of miR-1 for adaptation of gene expression during cardiac hypertrophy.

In this study, we report that knockdown of G3bp1 in cardiomyocytes results in inhibited expression of cardiac-enriched sarcomeric and cardiomyopathy-related genes, hence restricts growth-factor induced cardiomyocyte hypertrophy. On the other hand, there is increase in genes of Hippo, TNF and TGFβ signaling. We further confirm that hypertrophic effects of G3bp1 in cardiomyocytes are indeed mediated through its regulation of miR-1 levels in cardiomyocytes. Interestingly, expression of fusion protein G3bp1-Gfp in cardiomyocytes showed assembly of perinuclear aggregates, resembling stress granules. These results show that G3bp1 is required for the induction of hypertrophic transcriptome and development of cardiomyocyte hypertrophy.

1.2 Materials and Methods

1.2.1 Animals.

The work was done in accordance with US National Institute of Health *Guidelines for Care and Use of Laboratory Animals*. All animal protocols were approved by the Institutional Animal Care and Use Committee (IACUC) at the Rutgers New Jersey Medical School, Newark, NJ. Female Sprague Dawley rats with 1day old litter for isolation and culture of primary neonatal cardiomyocyte were purchased from Charles River, InC.

1.2.2 RNA-Seq Data Analysis.

Total RNA samples from isolated neonatal cardiomyocytes (3 independent cultures for each treatment, n=3) treated with ad-siLUC (Control) or ad-siG3bp1 were sent to Active Motif for high throughput RNA sequencing and bioinformatics analysis. Analysis steps adapted from the Data explanation sheet provided by Active Motif are briefly described. Directional poly-A RNAseq libraries were prepared and sequenced as PE42 (42-bp paired-end reads) on Illumina NextSeq 500. The reads were mapped to the genome using STAR algorithm. Alignment information for each read was stored in the BAM format. Fragment assignment included only read pairs that have both ends aligned, and pairs that have their two ends mapping to different chromosomes or mapping to same chromosome but on different strands were discarded. Gene annotations were obtained from Subread package. These annotations were originally from NCBI RefSeq database and then adapted by merging overlapping exons from the same gene to form a set of disjoint exons from each gene. Genes with the same Entrez gene identifiers were also merged into one gene. After obtaining the gene table containing fragment counts of genes, differential analysis to identify statistically significant differential genes was performed using DESeq2. The DESeq2 model internally corrects for library size using their median-of-ratios method. The gene table was used as input to perform the DESeq2's differential test. After a differential test has been applied to each gene except the ones with zero counts, the p-value of each gene was calculated and needed to be further adjusted to control the number of false positives among all discoveries at a proper level by multiple testing adjustments. DESeq2 by default filters out statistical tests that have low counts by independent filtering. It uses the average counts of each gene (i.e. baseMean), across all samples, as it's filter criterion, and it omits all genes with average normalized counts below a filtering threshold from multiple testing adjustment. Differential genes were detected by DESeq2 at 0.1 (or 10%) False Discovery Rate (FDR, or adjusted p-value).

The data is provided in CSV file that reports information for each gene along with DESeq2' results. Along with the p-values, the file reports adjusted p-value (padj) generated by Benjamini and Hochbergs' FDR procedure that reflects the proportion of false positives expected for a gene to be differential. There are two types of log2FCs included in the output. RawLog2FC which is the raw log2 fold change obtained from the replicate averages of normalized counts of the two comparison groups. However, directly using rawLog2FC to rank genes was not ideal because ratios are noisier when counts are low. To overcome this problem, we used a shrinkage method in DESeq2 to shrink the exaggerated log2 FCs for low counts and used shrunken Log2FC for downstream analysis. Using shrunkenLog2FC is more reliable to rank genes for quantitative conclusion than rawLog2FC. RNAseq data has been uploaded to GEO (**GSE184441**).

Heatmap generation, sorting and data analysis was performed using shrunkenLog2FC and adjusted p-value (padj) was used for significance ($P \leq 0.05$)

1.2.3 Functional annotation and GO terms.

Functional annotation was performed using Database for Annotation, Visualization and Integrated Discovery (DAVID) algorithm 6.8 [13] [14]. Gene ontology terms and Kyoto

Encyclopedia of Genes and Genome (KEGG) pathways [15] generated via DAVID are shown in Figures (top categories) and the complete list is shown as supplementary figures.

1.2.4 Neonatal Rat Ventricular Myocyte (NRVM) Culture and Treatments.

Neonatal cardiomyocytes were cultured as previously described [16]. Briefly, hearts from 1day old Sprague Dawley rats were isolated and dissociated. Enrichment of cardiac myocytes was performed using Percoll Gradient followed by differential pre-plating, to deplete any contaminating non-myocytes. Cells were plated in DMEM-F12 (High Glucose, with L-glutamine and HEPES) with 10% fetal bovine serum, after twenty-four hours medium was changed and cells were infected with recombinant adenoviruses (constructed using protocol as previously described by Dr. Frank Graham [17]) expressing shRNA against rat G3bp1 (NM_133565.1) or exogenous mouse G3bp1(NM_013716) from OriGene Technologies, Inc at the multiplicity of infection (MOI) of 10–20 particles /cell or as indicated. Similarly, adenoviruses were generated for expression of miR-1-2 (ad-miR-1) [8] and ‘miRNA eraser’ (anti-miR) was generated as described previously [18], for the knockdown of endogenous miR-1 (ad-anti-miR-1) [7].

1.2.5 Adult Mouse Ventricular Myocyte (AMVM) culture.

Adult mouse cardiac myocytes were isolated and cultured according to the simplified Langendorff-free method reported by Ackers-Johnson et. al. [19]. It relies mostly on ex vivo needle perfusion of left ventricle, which allows enzymatic dissociation of heart tissue. Dissociation was carried out by sequential injection of EDTA buffer, perfusion buffer and collagenase buffer and when the digestion became apparent the tissue was triturated gently and the resultant cell suspension was passed through a 100μm cell strainer. Single cell type fractions of physiologically normal cardiac myocytes were achieved by repeated gravity settling of the cell suspensions synchronized with sequential calcium reintroduction. Cells were plated at application dependent density on laminin 5μg/ml pre-coated tissue culture dishes and incubated in plating medium for 1 hour and further in culture medium. The cultured AMCs are treated similarly as NRVM, except the adenoviruses are added the same day as culture. ET-1 stimulation is done the following day for ~20hrs and the cells are fixed or collected for immunostaining or Western blotting, respectively.

1.2.6 Cellular fractionation and Western Blotting.

As described previously [16]. Cardiomyocytes were fractionated using Subcellular protein fractionation kit for cultured cells from Thermo Scientific (cat # 78840), as per the manufacturer provided protocol. Lysate was separated on gradient (4–12% gel) XT gels (Biorad), transferred to nitrocellulose membrane and probed with specific antibodies against G3bp1 (Millipore, 07-1801), Ankrd1 (Santacruz, SC-365056), Rassf1 (Invitrogen, PA5-102383), TFIIB/Gtf2b (Cell Signaling, 4169S), Anp/Nppa (Invitrogen 702539), Lamin A/C (Santacruz, SC-376248), a-actinin-mouse (ThermoFisher, MA1-22863), α-actinin-rabbit (Invitrogen, 701914), Gapdh (Cell Signaling, 97166), Turbo Gfp (ThermoFisher, PA5-22688) or Myosin, slow skeletal (Sigma, M8421).

1.2.7 Quantitative polymerase chain reaction (qPCR).

As described in [20]. Briefly, total RNA extracted from hearts or isolated cardiomyocytes was reverse transcribed using High-capacity cDNA reverse transcription kit (ThermoFisher). TaqMan assays sets were purchased from ThermoFisher Science (Life technologies) for Actc1 (Mm01333821_m1), Acta1 (Mm00808218_g1), Arrdc3 (Rn01757892_m1), Ckmt2 (Mm01285553_m1), G3bp1 (Mm00785370_s1), Nppa (Mm01255747_g1) and Rassf1 (Rn01445298_m1) for qPCR using QuantStudio3 (Life technologies). 18S was used as internal control and for normalization.

1.2.8 Immunocytochemistry.

Cells were fixed as described previously [8]. Cells were stained using anti-G3bp1(Millipore, 07-1801), anti-a-actinin-mouse (ThermoFisher, MA1-22863) or a-actinin-rabbit (Invitrogen, 701914), as indicated. Prolong Gold (Invitrogen, USA) used for mounting contains DAPI for nuclear staining.

1.2.9 Statistics.

RNA-Seq data and bioinformatics analysis done by Active Motif, as described in RNAseq section. Calculation of significance between 2 groups was performed using an unpaired, 2-tailed Students *t* test (Excel software). All experiments were repeated minimum of three times, unless indicated and presented as average with SEM, $p<0.05$ was considered significant.

1.3 Results

1.3.1 Knockdown of G3bp1 results in inhibition of cardiac-enriched genes in cardiomyocytes.

We have shown that G3bp1 expression increases during cardiac hypertrophy and it regulates miR-1 biogenesis via the consensus sequence in miR-1-2 stem-loop [7]. Therefore, to examine the impact of G3bp1 on cardiac transcriptome, we performed RNAseq on NRVM infected with adenovirus expressing short hairpin RNA against G3bp1 (ad-siG3bp1) or control (ad-siLUC). RNA seq data from these cardiac myocytes reveal that knockdown of endogenous G3bp1 results in differential expression of 1140 genes, of which 658 show an increase of at least 2fold (Log2FC>1) while 482 genes are downregulated (Log2FC<1) compared to control cardiomyocytes (Fig 1A and B). Heatmap displays the differential regulation of these 1140 genes between cardiomyocytes treated with ad-siG3bp1 or control (ad-siLUC) (Fig1B). We categorized the differentially regulated genes for gene ontology (GOTERMS) and related signaling pathways (KEGG) using Database for Annotation, Visualization and Integrated Discovery (DAVID). GOTERM identified genes with significant increase with siG3bp1 as those involved in transcription regulation, cellular response to interleukin-1, TNF and inflammatory, along with skeletal muscle development and potassium ion transport (Fig 1D). Fig 2E lists the top ranked pathways identified by KEGG analysis and includes genes of TNF signaling pathway, cytokine receptor interactions, TGF-β and MAPK signaling pathways, and regulation of the Hippo pathway (Fig 1E) that are significantly increased. On the other hand, significant decrease with

knockdown of G3bp1 is observed in mostly cardiac-enriched genes. GOTERMS categorized these genes as those involved in cardiac muscle contraction, cardiac action potential, heart development and sarcomeric organization (Fig 1F). KEGG pathway analysis shows genes associated with pathways involved in calcium handling, adrenergic signaling, hypertrophic and dilated cardiomyopathy (Fig 1G). In Fig 1H, heatmap generated from the Gene Set Enrichment Analysis (GSEA), displays the change in expression pattern of genes that play a role in cardiac muscle contraction between siLUC and siG3bp1 treated cardiomyocytes (Fig 1H and Supp Fig S1). Complete list of categorized KEGG pathways and GOTERMS is included in supplementary figures (Supp Fig S2). Fig 1I and 1J are integrated genome viewer (IGV) screenshots of representative genes displaying the alignment of RNAseq reads onto the rat genome of Nppb, Nppa and Actc1 as genes that show a decrease (Fig 1I) and Pdk4, Arrdc3 and Rassf1 for genes with significant increase (Fig 1J) in transcript abundance with siG3bp1 compared to siLUC. These results suggests that G3bp1 plays an essential role in the maintenance and/or expression of cardiac-enriched genes, especially, those involved in regulating cardiac contraction and growth.

1.3.2 G3bp1 is required for growth-factor induced hypertrophy in isolated NRVM.

To examine the role and contribution of G3bp1 in regulating gene expression in cardiac myocytes undergoing growth-factor induced hypertrophy, we infected NRVM with ad-siG3bp1 or control (ad-siLUC) in absence or presence of endothelin 1 (ET1). Selected representative genes from the RNAseq were used for qPCR and western blotting (Fig 2A). Ad-siG3bp1 infection resulted in ~70% reduction in transcript abundance of G3bp1, which inhibited ET-1 induced increase in G3bp1 protein expression (Fig 2B and 2C). We validated the expression of selected genes listed in Fig 2A, including hypertrophic makers like Nppa (Anf), cardiac-enriched sarcomeric genes like Actc1 (cardiac actin) and mitochondrial creatinine kinase (Ckmt2), which show decrease with the knockdown of G3bp1 in quiescent and ET-1 stimulated conditions. Similarly, we confirmed increased in Arrdc3 (arrestin domain containing 3) expression, as observed with the knockdown of G3bp1 in RNAseq (Fig 2B). Ankrd1 (Carp), although just showed differential change of −0.76 on Log2FC, we observed significant decrease in protein expression with siG3bp1 in cardiomyocytes stimulated with ET-1 (Fig 2C). Further, knockdown of G3bp1 restricted ET-1 induced increase in cardiomyocyte size in dose dependent manner (Fig 2D). Similar effects were seen when cardiomyocytes were treated with an α_1- receptor agonist, phenylephrine (PE) (Fig 2E, 2F and Fig S3A). We further validated the specificity of siG3bp1 mediated transcriptome changes by supplementing exogenous G3bp1 in cardiomyocytes treated with ad-siG3bp1. As shown in supplementary Fig S3A and S3B, normalizing G3bp1 levels rescues expression profile of selected genes (Fig S3A and 3B). These results indicate that G3bp1 regulates cardiomyocyte growth and suggest that G3bp1 is required for the adaptation of gene expression and development of hypertrophy.

1.3.3 G3bp1 – miR-1 axis regulates cardiomyocyte hypertrophy.

G3bp1 regulates miR-1 expression levels in cardiomyocytes [7]. Interestingly, in an independent study we have shown that miR-1 controls global gene transcription in cardiac myocytes, especially, expression of inducible and cardiac-enriched genes by targeting Gtf2b and Cdk9, and inhibits induction of hypertrophy [9]. Thus, to examine if G3bp1 mediates

its downstream effects on the transcription of these genes and cardiomyocyte hypertrophy in miR-1 dependent manner, we co-infected NRVM with ad-siG3bp1 and ad-miR-1 eraser (anti-miR-1) or control (ad-siLUC) in absence or presence of ET-1. As shown in Fig 3A, knockdown of endogenous miR-1 and G3bp1 together rescued the expression levels of Nppa (Anf), Actc1, Arrdc3 and Rassf1, compared to expression seen with knockdown of G3bp1 in quiescent and ET-1 stimulated cardiomyocytes. (Fig 3A). Rassf1, an inhibitor of the active Hippo signaling that has been shown to ameliorate cardiac hypertrophy [21] is seen significantly increased with siG3bp1 in RNAseq (Fig 1C) and confirmed by qPCR (Fig 3A), suggesting that G3bp1 might be regulating Hippo pathways via miR-1 to regulate cardiomyocyte hypertrophy. Western blotting confirm that while siG3bp1 results in inhibited expression of Ankrd1 (Fig 1A), simultaneous knockdown of miR-1 partially rescues its expression levels (Fig 3B). Ankrd1, which encodes for cardiac ankyrin repeat protein (CARP), a transcriptional target of active Hippo signaling [22], has been shown to promote cardiac hypertrophy [23] and involved in development of dilated cardiomyopathy [24]. Interestingly, cytosolic Rassf1 levels is seen increased with the inhibition of G3bp1, while nuclear fractions show decrease in presence of ET-1, with or without siG3bp1 (Fig 3B). Along with the transcriptional profile, knockdown of endogenous miR-1 levels by anti-miR-1 also reverse the restricted hypertrophy phenotype observed with siG3bp1 in cardiomyocytes stimulated with ET-1 (Fig 3C and D). Interestingly, although anti-miR-1 is sufficient for upregulation of Nppa and Actc1 expression, it is not sufficient for an increase in cardiomyocyte size. No change is seen in the expression of Arrdc3 or Rassf1, thus suggesting that these genes through regulation of Hippo signaling contribute towards cardiomyocyte growth. Thus, as previously reported, downregulation of miR-1 although required, is not sufficient for the induction and development of hypertrophy [25].

Next, to determine if G3bp1 expression is sufficient for induction of transcriptional and hypertrophic phenotype, we expressed G3bp1-tGfp in NRVM in absence or presence of ET-1. We validated the expression of the adenoviral constructs, tGfp (control) and G3bp1-tGfp in cardiomyocytes (Fig 4A). To examine the G3bp1–miR-1 axis in cardiomyocyte, we co-expressed exogenous miR-1 with G3bp1-tGfp in NRVMs. Exogenous G3bp1, was insufficient for significant change in transcriptome, as measured by transcript abundance of selected genes including Nppa, Ckmt2 and Rassf1, although, an increase is observed in Actc1 transcript. As expected, expression of miR-1 resulted in inhibited expression of Nppa and Actc1, while an increase was seen in Arrdc3 and Rassf1. However, co-expression of G3bp1 with miR-1 rescues the inhibitory effects of miR-1 with respect to Nppa and Actc1, but, a partial inhibition is seen with miR-1 induced increase Arrdc3 and Rassf1 (Fig 4B). These data indicate that G3bp1 through its posttranscriptional regulation of miR-1 regulates expression of transcriptome that is required for cardiomyocyte hypertrophy.

Neonatal cardiomyocyte cultures are undergoing postnatal cardiac hypertrophy, even though these cultures are maintained in growth-free medium before supplementation of ET-1 for induction of hypertrophy. Thus, to examine that G3bp1–miR-1 signaling is intact in adult cardiomyocytes and regulates development of cardiomyocyte hypertrophy, we cultured adult mouse ventricular cardiomyocytes (AMVM) and validated the expression of our adenoviral vectors (Fig 5C and 5D). As shown in Fig 5A, siG3bp1 or anti-miR-1 were insufficient to elicit anti-hypertrophic or hypertrophic response under quiescent conditions,

respectively. However, siG3bp1 restricted ET-1 induced increase in cardiomyocyte size that was rescued in the presence of anti-miR-1 (Fig 5A and 5B). Similar to neonatal cardiomyocytes, overexpression of G3bp1 prevents miR-1 mediated inhibition of ET-1 induced cardiomyocyte hypertrophy (Fig 5E and F). Interestingly, expression of exogenous G3bp1 showed perinuclear cytoplasmic accumulation (Fig 5E, 5G and Supp Fig S4). Similar accumulations have been shown in other cell types with exogenous G3bp1 expression or induced stress [4], [26], and have been identified as stress granules, which serve triage sites for mRNAs [27], [28]. The significance and the role of these stress granule assembly with G3bp1 overexpression in cardiomyocytes needs further examination and characterization.

1.4 Conclusion

Based on our transcriptome data with the knockdown of G3bp1 and *in vitro* characterization of the G3bp1–miR-1 axis we conclude that G3bp1 through its regulation of miR-1 levels controls the expression of genes that are required for the development of cardiomyocyte hypertrophy.

1.5 Discussion

In this study we show that G3bp1, a ubiquitously expressed RNA binding protein is required for cardiomyocyte growth. We extend our work from previous report [7] and show that G3bp1 through its regulation of miR-1 expression controls growth-factor induced hypertrophy. Using high throughput transcriptome sequencing, we identified genes that are differentially regulated with the knockdown of G3bp1 and contribute in the development of cardiomyocyte hypertrophy. G3bp was first identified as GAP binding protein in growing hamster fibroblast cells (ER22), and this interaction was Ras-GTP dependent, where activation of Ras was essential for G3bp-GAP association [1]. Molecular cloning and sequencing showed presence of two conserved RNA binding motifs and RGG rich domain, 3’ to an acidic domain, suggesting that G3bp could belong to family of hnRNPs, and categorized as a ribonucleoprotein [1]. G3bp was shown to harbor an endoribonuclease activity that was dependent on its phosphorylation status, where RasGAP mediated modification of specific serine residues in the acidic domain could dictate G3bp cellular localization and nuclease activity [2] [3]. Following on its role as a nuclease, Tourriere et. al. reported that the activity was substrate specific and G3bp associated with poly(A)$^{+}$ transcripts encoding a consensus sequence ACCCA(A/U)(A/C)(C/G)G(C/A)AG in their 3’UTR or coding region, with G3bp cleavage site at CA dinucleotides. Using BLAST, the study identified several genes in humans, mouse and rodents that harbored the consensus sequence, including cyclin dependent kinase 9 (Cdk9), lanosterol synthase (Lss), interferon regulatory factor 7 (Irf7) and cornified envelop precursor (periplakin or Ppl) [3], these genes are also increased in our RNAseq data in cardiomyocytes with the knockdown of G3bp1 (Supp FigS5), validating site specific endoribonuclease mode of action of G3bp1. While working on the role and regulation of miR-1 in heart, we identified G3bp consensus sequence in its stem-loop with few mismatches, suggesting that G3bp1 could be involved in miR-1 processing and maturation. Aligning human, mouse and rat miR-1-1 and miR-1-2 stem-loop against G3bp consensus sequence revealed mismatch in the CA dinucleotide in miR-1-1, where C was replaced by G. Interestingly, decrease in the expression of mouse pre-

miR-1-2 was seen in hypertrophy and with exogenous G3bp1 expression, while pre-miR-1-1 levels did not change, indicating that G3bp1 selectively decreased pre-miR-1-2 transcript levels, resulting in ~50% decrease in mature miR-1 [7],[8]. Previously we have shown that downregulation of miR-1 is required for the cardiac hypertrophy [8],[25], which through de-repression of its target, GTF2B, regulates RNA pol II recruitment at inducible and cardiac-enriched gene promoters [29], [9]. Thus, our RNAseq results confirm the posttranscriptional regulation of miR-1 by G3bp1, and dependent downstream effects on transcriptome in cardiomyocytes undergoing hypertrophy. Along with its nuclease function, G3bp has been shown to be involved in nucleating the assembly of cytoplasmic RNA-protein aggregates, called stress granules [4].

Stress granules act as docking sites for transcripts that are stalled from translation under stress conditions, the fate of which is decided based on the type and duration of the induced stress [6]. These membrane-less aggregations are highly dynamic, and hence, the associated transcripts and RNPs are still being characterized, which would depend on the cell type and the nature of the stress. Early characterization studies identified RNPs that are essential for the nucleation of stress granules and include RNA binding proteins TIA-1 and TIAR, along with G3bp [5] [30] [4]. Two G3bp isoforms have been identified, G3bp (G3bp1) and G3bp2, both of which play a role in stress granule assembly [26]. Interestingly, expression of exogenous G3bp has been shown sufficient for the formation of these granules, even in the absence of stress, we see similar aggregations in isolated cardiomyocytes with exogenous G3bp1 (Fig 5E, 5G and Supp Fig S2). Initial studies associated these granule assembly with change in the phosphorylation status of serine 149 in the acidic domain of G3bp1 [4], however, a later study showed that an unidentified mutation at serine 99, where serine was changed to proline (S99P) in the constructs could have been responsible for the formation of these structures [31]. Recently, presence of stress granules has been shown in paced atrial cardiomyocytes [32], however, the regulation and function of G3bp1 induced stress granules, it's dynamics and contents in cardiomyocytes need further examination to decipher the significance and implications in heart disease. It would be interesting to examine if G3bp1 associates with pre-miR-1-1 in hypertrophying cardiomyocytes via partial consensus sequence but does not cleave the stem-loop due to the change in CA dinucleotide to GA [7], and instead recruits it to stress granules. Recently, Decitabine and Imatinib, two FDA approved drugs for treatment of myelodysplastic syndromes [33] have been identified as modulators of G3bp1/2 with potential therapeutic value for controlling SARS-CoV-2 infection [34]. Nucleocapsid protein N of SARS-CoV-2 interacts with G3bp proteins and inhibits stress granule assembly, thus alters the stress response and favors viral propagation [35]. These studies underscore the role of G3bp and stress granules in physiological cellular responses to stress. In this study, we show that G3bp1 via miR-1 regulates transcriptome during hypertrophic stress, which is required for development of compensatory hypertrophy. Further, with the identification of these FDA approved drugs in regulating G3bp1 levels and function, it would be interesting to study their effects on G3bp1 function in quiescent hearts, and during cardiac hypertrophy and failure.

Global knockout of G3bp1 results in neonatal lethality, with widespread apoptotic cell death in the central nervous system. G3bp deficiency caused fetal growth retardation, where the embryos displayed dorsal truncation, stunted tails and cranial defects. Characterization

of MEFs from these mice showed defects in proliferation, with differential expression of genes mostly involved in proliferation and differentiation [36]. Our RNAseq data, with knockdown of G3bp1 shows similar dysregulation in most of the listed genes with siG3bp1, like Lasp1, Fhl1, Ldb3, Plac8, including structural genes like actin, alpha 1 (Acta1) and cardiac ankyrin repeat protein MCARP (Ankrd1). On the other hand, while the expression of Growth arrest genes; Gas2 and Gas5 is seen significantly upregulated in G3bp1KO MEFs, we observed slight decrease in their expression. This could be due to difference in cell type, with cardiomyocytes being terminally differentiated vs. proliferating fibroblasts. G3bp1 in association with RasGAP and Filamin C has been shown to regulate myocyte growth, through its interaction with Cdk7 and Cdk9 transcripts, both these genes are involved in RNA pol II phosphorylation and active transcription [37]. We show that knockdown of endogenous G3bp1 results in inhibited cardiomyocyte hypertrophy, with restricted expression of inducible and cardiac-enriched genes like, Anf (Nppa) and cardiac actin (Actc1), respectively. On the other hand, we observe increase in genes of Hippo pathway, along with induction of genes involved in TNF and TGF-b signaling. Hippo signaling has been well characterized as regulator of cell proliferation and organ growth [38],[39],[40]. Rassf1, negative regulator of Hippo pathway activation has been shown as novel regulator of cardiac hypertrophy [41],[21]. Similarly, Arrdc3 has been shown to facilitate YAP1 degradation [42]. Increase in Rassf1 and Arrdc3 expression we observe with siG3bp1 or miR-1 expression suggest inhibition of the Hippo signaling pathway, which might be contributing to inhibition of ET-1 induced cardiomyocyte hypertrophy. As expected, we see differential regulation of several of the known targets of Hippo signaling in cardiomyocytes with inhibition of siG3bp1 (Supp Fig S6). Yap/Tead1 complex has been shown as repressor of cardiac toll-like receptors genes [43], which are seen increased significantly in RNAseq data with siG3bp1. Similarly, we observe inhibition of the several target genes, the transcription of which is regulated by Hippo signaling like Ankrd1, Rheb, Bcl2, Pitx2 [44], [22].

In this study we only report genes that are differentially regulated (2 fold) by G3bp1 inhibition, however, since G3bp1 is also involved in assembly of stress granules and mRNA triage, it may be involved in stabilization of transcripts, like reported for Cdk7 mRNA [37]. Thus, these genes, which are not expected not show a differential regulation were not included in the study. Nevertheless, our data did show that G3bp1 significantly regulates the expression of cardiac-enriched genes and is required for the inducible genes during hypertrophic stimulation. We conclude that G3bp1, a unique protein, with dual phosphorylation dependent functionality might be playing an essential role in maintaining cardiac homeostasis and contribute to development of compensatory cardiomyocyte hypertrophy.

Supplementary Material

Refer to Web version on PubMed Central for supplementary material.

Acknowledgements:

We thank Dr. Abdellatif, Professor in Department of Cell Biology and Molecular Medicine for providing Ad-siG3bp1 (adenovirus) for in vitro knockdown experiments, and for the support. We also thank Dr. Sadoshima, Chair of department of Cell Biology and Molecular Medicine, Rutgers New Jersey Medical School for support.

Funding:

This work was supported by National Heart, Lung, and Blood Institute (NHLBI) of National Institute of Health (NIH) funding to the corresponding author (R01HL128799 and R01HL150059).

Bibliography

1. Parker F, Maurier F, Delumeau I, Duchesne M, Faucher D, Debussche L, et al. A Ras-GTPase-activating protein SH3-domain-binding protein. Mol Cell Biol. 1996;16(6):2561–9. [PubMed: 8649363]
2. Gallouzi IE, Parker F, Chebli K, Maurier F, Labourier E, Barlat I, et al. A novel phosphorylation-dependent RNase activity of GAP-SH3 binding protein: a potential link between signal transduction and RNA stability. Mol Cell Biol. 1998;18(7):3956–65. [PubMed: 9632780]
3. Tourriere H, Gallouzi IE, Chebli K, Capony JP, Mouaikel J, van der Geer P, et al. RasGAP-associated endoribonuclease G3Bp: selective RNA degradation and phosphorylation-dependent localization. Mol Cell Biol. 2001;21(22):7747–60. [PubMed: 11604510]
4. Tourriere H, Chebli K, Zekri L, Courselaud B, Blanchard JM, Bertrand E, et al. The RasGAP-associated endoribonuclease G3BP assembles stress granules. J Cell Biol. 2003;160(6):823–31. [PubMed: 12642610]
5. Kedersha NL, Gupta M, Li W, Miller I, Anderson P. RNA-binding proteins TIA-1 and TIAR link the phosphorylation of eIF-2 alpha to the assembly of mammalian stress granules. J Cell Biol. 1999;147(7):1431–42. [PubMed: 10613902]
6. Kedersha N, Anderson P. Stress granules: sites of mRNA triage that regulate mRNA stability and translatability. Biochem Soc Trans. 2002;30(Pt 6):963–9. [PubMed: 12440955]
7. He M, Yang Z, Abdellatif M, Sayed D. GTPase Activating Protein (Sh3 Domain) Binding Protein 1 Regulates the Processing of MicroRNA-1 during Cardiac Hypertrophy. PLoS One. 2015;10(12):e0145112. Epub 2015/12/18. doi: 10.1371/journal.pone.0145112. [PubMed: 26675618]
8. Sayed D, Hong C, Chen IY, Lypowy J, Abdellatif M. MicroRNAs play an essential role in the development of cardiac hypertrophy. Circ Res. 2007;100(3):416–24. [PubMed: 17234972]
9. Sayed D, Yang Z, He M, Pfleger JM, Abdellatif M. Acute targeting of general transcription factor IIB restricts cardiac hypertrophy via selective inhibition of gene transcription. Circ Heart Fail. 2015;8(1):138–48. [PubMed: 25398966]
10. Ikeda S, Kong SW, Lu J, Bisping E, Zhang H, Allen PD, et al. Altered microRNA expression in human heart disease. Physiol Genomics. 2007;31(3):367–73. [PubMed: 17712037]
11. Ikeda S, He A, Kong SW, Lu J, Bejar R, Bodyak N, et al. MicroRNA-1 negatively regulates expression of the hypertrophy-associated calmodulin and Mef2a genes. Mol Cell Biol. 2009;29(8):2193–204. [PubMed: 19188439]
12. Sucharov CC, Kao DP, Port JD, Karimpour-Fard A, Quaife RA, Minobe W, et al. Myocardial microRNAs associated with reverse remodeling in human heart failure. JCI Insight. 2017;2(2):e89169. Epub 2017/02/01. doi: 10.1172/jci.insight.89169. [PubMed: 28138556] outstanding shares) in Miragen Therapeutics, and M.R. Bristow is member of the Miragen Scientific Advisory Board.
13. Huang da W, Sherman BT, Lempicki RA. Bioinformatics enrichment tools: paths toward the comprehensive functional analysis of large gene lists. Nucleic Acids Res. 2009;37(1):1–13. [PubMed: 19033363]
14. Huang da W, Sherman BT, Lempicki RA. Systematic and integrative analysis of large gene lists using DAVID bioinformatics resources. Nat Protoc. 2009;4(1):44–57. [PubMed: 19131956]

15. Kanehisa M, Goto S, Sato Y, Furumichi M, Tanabe M. KEGG for integration and interpretation of large-scale molecular data sets. Nucleic Acids Res. 2012;40(Database issue):D109–14. Epub 2011/11/15. doi: 10.1093/nar/gkr988. [PubMed: 22080510]

16. Severinova E, Alikunju S, Deng W, Dhawan P, Sayed N, Sayed D. Glucocorticoid Receptor-Binding and Transcriptome Signature in Cardiomyocytes. J Am Heart Assoc. 2019;8(6):e011484. Epub 2019/03/15. doi: 10.1161/jaha.118.011484. [PubMed: 30866692]

17. Graham FL PL. Methods in Molecular Biology. The Humana Press Inc, Clifton, NJ. 1991:109–28.

18. Sayed D, Rane S, Lypowy J, He M, Chen IY, Vashistha H, et al. MicroRNA-21 targets Sprouty2 and promotes cellular outgrowths. Mol Biol Cell. 2008;19(8):3272–82. [PubMed: 18508928]

19. Ackers-Johnson M, Li PY, Holmes AP, O'Brien SM, Pavlovic D, Foo RS. A Simplified, Langendorff-Free Method for Concomitant Isolation of Viable Cardiac Myocytes and Nonmyocytes From the Adult Mouse Heart. Circ Res. 2016;119(8):909–20. Epub 2016/08/10. doi: 10.1161/circresaha.116.309202. [PubMed: 27502479]

20. Alikunju S, Severinova E, Yang Z, Ivessa A, Sayed D. Acute NelfA knockdown restricts compensatory gene expression and precipitates ventricular dysfunction during cardiac hypertrophy. J Mol Cell Cardiol. 2020;142:93–104. Epub 2020/04/13. doi: 10.1016/j.yjmcc.2020.04.007. [PubMed: 32278832]

21. Oceandy D, Pickard A, Prehar S, Zi M, Mohamed TM, Stanley PJ, et al. Tumor suppressor Ras-association domain family 1 isoform A is a novel regulator of cardiac hypertrophy. Circulation. 2009;120(7):607–16. Epub 2009/08/05. doi: 10.1161/circulationaha.109.868554. [PubMed: 19652091]

22. Chen X, Li Y, Luo J, Hou N. Molecular Mechanism of Hippo-YAP1/TAZ Pathway in Heart Development, Disease, and Regeneration. Frontiers in physiology. 2020;11:389. Epub 2020/05/12. doi: 10.3389/fphys.2020.00389. [PubMed: 32390875]

23. Zhong L, Chiusa M, Cadar AG, Lin A, Samaras S, Davidson JM, et al. Targeted inhibition of ANKRD1 disrupts sarcomeric ERK-GATA4 signal transduction and abrogates phenylephrine-induced cardiomyocyte hypertrophy. Cardiovasc Res. 2015;106(2):261–71. Epub 2015/03/15. doi: 10.1093/cvr/cvv108. [PubMed: 25770146]

24. Moulik M, Vatta M, Witt SH, Arola AM, Murphy RT, McKenna WJ, et al. ANKRD1, the gene encoding cardiac ankyrin repeat protein, is a novel dilated cardiomyopathy gene. Journal of the American College of Cardiology. 2009;54(4):325–33. Epub 2009/07/18. doi: 10.1016/j.jacc.2009.02.076. [PubMed: 19608030]

25. Sayed D, Abdellatif M. MicroRNAs in Development and Disease. Physiol Rev. 2011;91(3):827–87. [PubMed: 21742789]

26. Matsuki H, Takahashi M, Higuchi M, Makokha GN, Oie M, Fujii M. Both G3BP1 and G3BP2 contribute to stress granule formation. Genes Cells. 2013;18(2):135–46. [PubMed: 23279204]

27. Lopez de Silanes I, Galban S, Martindale JL, Yang X, Mazan-Mamczarz K, Indig FE, et al. Identification and functional outcome of mRNAs associated with RNA-binding protein TIA-1. Mol Cell Biol. 2005;25(21):9520–31. [PubMed: 16227602]

28. Kedersha N, Stoecklin G, Ayodele M, Yacono P, Lykke-Andersen J, Fritzler MJ, et al. Stress granules and processing bodies are dynamically linked sites of mRNP remodeling. J Cell Biol. 2005;169(6):871–84. [PubMed: 15967811]

29. Sayed D, He M, Yang Z, Lin L, Abdellatif M. Transcriptional regulation patterns revealed by high resolution chromatin immunoprecipitation during cardiac hypertrophy. J Biol Chem. 2013;288(4):2546–58. [PubMed: 23229551]

30. Kedersha N, Cho MR, Li W, Yacono PW, Chen S, Gilks N, et al. Dynamic shuttling of TIA-1 accompanies the recruitment of mRNA to mammalian stress granules. J Cell Biol. 2000;151(6):1257–68. [PubMed: 11121440]

31. Panas MD, Kedersha N, Schulte T, Branca RM, Ivanov P, Anderson P. Phosphorylation of G3BP1-S149 does not influence stress granule assembly. J Cell Biol. 2019;218(7):2425–32. Epub 2019/06/07. doi: 10.1083/jcb.201801214. [PubMed: 31171631]

32. Dong G, Liang F, Sun B, Wang C, Liu Y, Guan X, et al. Presence and function of stress granules in atrial fibrillation. PLoS One. 2019;14(4):e0213769. Epub 2019/04/04. doi: 10.1371/journal.pone.0213769. [PubMed: 30943206]

33. Bryan J, Jabbour E, Prescott H, Garcia-Manero G, Issa JP, Kantarjian H. Current and future management options for myelodysplastic syndromes. Drugs. 2010;70(11):1381–94. Epub 2010/07/10. doi: 10.2165/11537920-000000000-00000. [PubMed: 20614946]
34. Ali N, Prasad K, AlAsmari AF, Alharbi M, Rashid S, Kumar V. Genomics-guided targeting of stress granule proteins G3BP1/2 to inhibit SARS-CoV-2 propagation. Int J Biol Macromol. 2021;190:636–48. Epub 2021/09/14. doi: 10.1016/j.ijbiomac.2021.09.018. [PubMed: 34517025]
35. Nabeel-Shah S, Lee H, Ahmed N, Burke GL, Farhangmehr S, Ashraf K, et al. SARS-CoV-2 nucleocapsid protein binds host mRNAs and attenuates stress granules to impair host stress response. iScience. 2022;25(1):103562. Epub 2021/12/14. doi: 10.1016/j.isci.2021.103562. [PubMed: 34901782]
36. Zekri L, Chebli K, Tourriere H, Nielsen FC, Hansen TV, Rami A, et al. Control of fetal growth and neonatal survival by the RasGAP-associated endoribonuclease G3BP. Mol Cell Biol. 2005;25(19):8703–16. [PubMed: 16166649]
37. Lypowy J, Chen IY, Abdellatif M. An alliance between Ras GTPase-activating protein, filamin C, and Ras GTPase-activating protein SH3 domain-binding protein regulates myocyte growth. J Biol Chem. 2005;280(27):25717–28. [PubMed: 15886195]
38. Wu S, Huang J, Dong J, Pan D. hippo encodes a Ste-20 family protein kinase that restricts cell proliferation and promotes apoptosis in conjunction with salvador and warts. Cell. 2003;114(4):445–56. Epub 2003/08/28. doi: 10.1016/s0092-8674(03)00549-x. [PubMed: 12941273]
39. Udan RS, Kango-Singh M, Nolo R, Tao C, Halder G. Hippo promotes proliferation arrest and apoptosis in the Salvador/Warts pathway. Nat Cell Biol. 2003;5(10):914–20. Epub 2003/09/23. doi: 10.1038/ncb1050. [PubMed: 14502294]
40. Huang J, Wu S, Barrera J, Matthews K, Pan D. The Hippo signaling pathway coordinately regulates cell proliferation and apoptosis by inactivating Yorkie, the Drosophila Homolog of YAP. Cell. 2005;122(3):421–34. Epub 2005/08/13. doi: 10.1016/j.cell.2005.06.007. [PubMed: 16096061]
41. Polesello C, Huelsmann S, Brown NH, Tapon N. The Drosophila RASSF homolog antagonizes the hippo pathway. Curr Biol. 2006;16(24):2459–65. Epub 2006/12/19. doi: 10.1016/j.cub.2006.10.060. [PubMed: 17174922]
42. Xiao J, Shi Q, Li W, Mu X, Peng J, Li M, et al. ARRDC1 and ARRDC3 act as tumor suppressors in renal cell carcinoma by facilitating YAP1 degradation. Am J Cancer Res. 2018;8(1):132–43. Epub 2018/02/09. [PubMed: 29416926]
43. Gao Y, Sun Y, Ercan-Sencicek AG, King JS, Akerberg BN, Ma Q, et al. YAP/TEAD1 Complex Is a Default Repressor of Cardiac Toll-Like Receptor Genes. Int J Mol Sci. 2021;22(13). Epub 2021/07/03. doi: 10.3390/ijms22136649.
44. Totaro A, Panciera T, Piccolo S. YAP/TAZ upstream signals and downstream responses. Nat Cell Biol. 2018;20(8):888–99. Epub 2018/07/28. doi: 10.1038/s41556-018-0142-z. [PubMed: 30050119]

Highlights

- Posttranscriptional gene regulation plays an essential role in cardiac hypertrophy
- RNA binding proteins and microRNAs, posttranscriptionally regulate gene expression
- G3bp1 through microRNA-1 levels controls cardiomyocyte hypertrophic transcriptome
- G3bp is required for accommodation of gene expression and cardiomyocyte hypertrophy

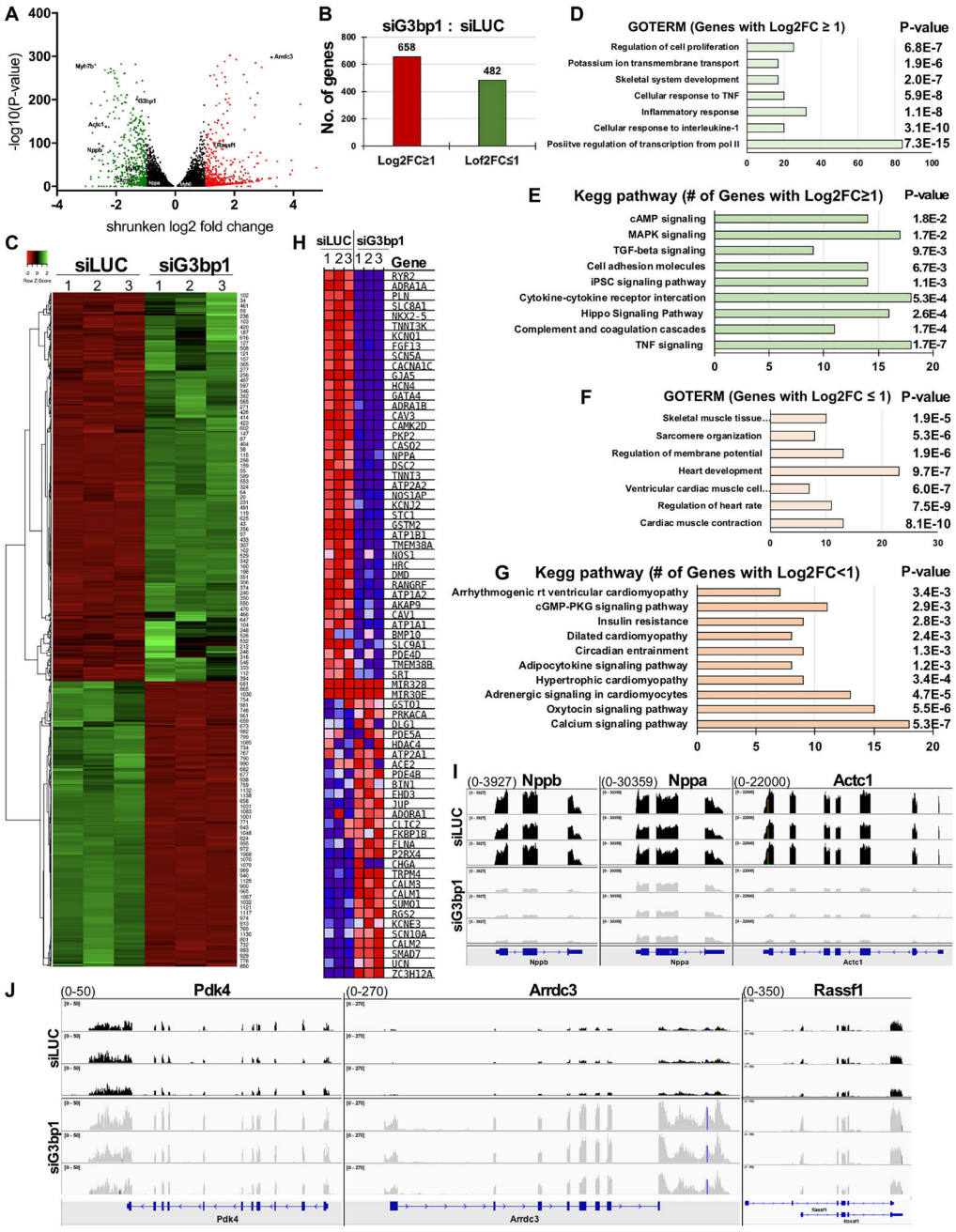

Figure 1.

Knockdown of endogenous G3bp1 in neonatal cardiomyocytes inhibits expression of cardiac-enriched genes. **A**. Volcano plot represents the differential expression of genes, with 2fold change in levels (Log2FC of 1). Each individual spot represents a gene. Selected genes are highlighted and labelled. **B**. Graph shows the number of genes that show significant change in expression with ad-siG3bp1 compared to ad-siLUC. **C**. Heatmap displays the 1140 differentially regulated genes in cardiomyocytes treated with ad-siG3bp1 vs control (ad-siLUC). Heatmap was generated using HeatMapper, with Complete linkage clustering method and Pearson method for distance measurement. RNAseq data included n=3 for each

treatment. **D** and **E**. Graphs lists genes identified by GOTERM and KEGG pathway analysis using DAVID that show an increase (>2fold, Log2FC≥1) change in expression with siG3bp1 vs. control (siLUC), respectively. **F** and **G**. Graphs list genes identified by GOTERM and KEGG pathway analysis that show decrease (2fold, Log2FC≤1) in expression with siG3bp1 vs. control (siLUC), respectively. **H**. Heatmap displays the change in expression of genes categorized as those involved in cardiac contraction by GSEA analysis, which used MSigDB's C5 (GO gene set) collection, with siLUC vs. siG3bp1 treatments. Red indicates increase, blue indicates decrease, with intensity of the colors proportional to the change. **I**. Integrated genomic viewer screenshots of selected, representative genes showing mRNA alignment onto the rat genome displaying the decrease in abundance with siG3bp1 (grey) vs. siLUC (black). **J**. Integrated genomic viewer screenshots of selected representative genes showing mRNA alignment onto the rat genome displaying the increase in abundance with siG3bp1 (grey) vs. siLUC (black). DAVID stands for Database for Annotation, Visualization and Integrated Discover; Log2FC, log2-fold change.

A

Gene ID	Gene Symbol	Chr	Length	siLUC-1	siLUC-2	siLUC-3	siG3bp1-1	siG3bp1-2	siG3bp1-3	shrunkenLFC siG3bp1/siLUC	padj siG3bp1/siLUC
10588	Actc1	chr3	1489	231841	240768	197163	41619	41472	44619	-2.35	1.65E-138
8182	Ckmt2	chr2	1198	362	347	352	140	117	126	-1.41	4.34E-25
2770	G3bp1	chr10	6548	8001	8506	8369	3290	3461	3304	-1.3	2.01E-201
6049	Myh7	chr15	5923	235110	282920	233576	109516	109844	111629	-1.16	1.03E-35
13207	Nppa	chr5	814	141702	160852	122411	68156	66242	79953	-0.95	5.45E-11
2181	Ankrd1	chr1	1742	90904	100012	87096	53961	53648	55228	-0.76	1.86E-63
12093	Gapdh	chr4	1273	26531	26478	25990	29927	31087	30613	0.22	7.97E-11
15916	Rassf1	chr8	1948	1307	1175	1126	2874	3128	3056	1.32	1.28E-97
11354	Pdk4	chr4	1425	121	147	121	349	356	368	1.42	2.35E-25
8163	Arrdc3	chr2	1245	225	242	215	2085	2479	2168	3.26	6.71E-299

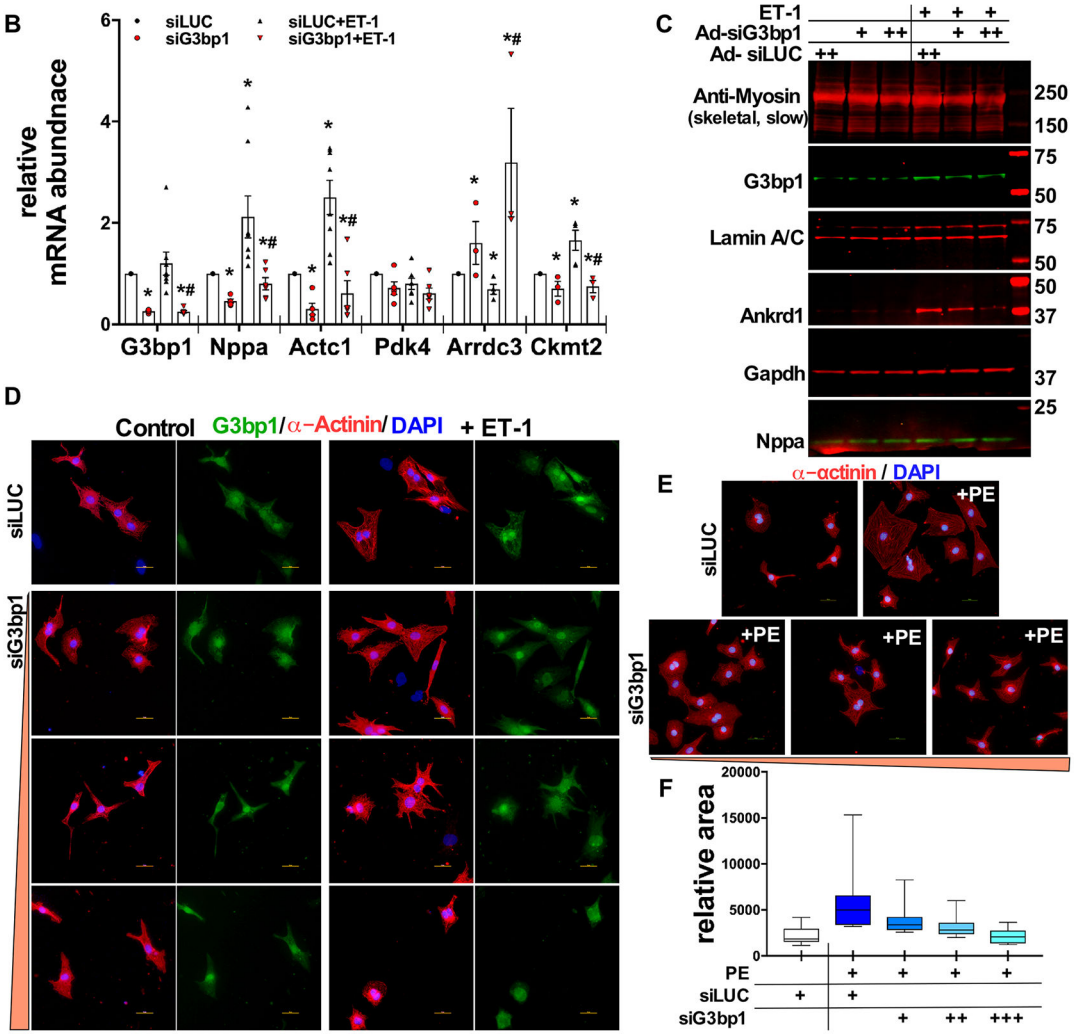

Figure 2.

Knockdown of G3bp1 inhibits growth-factor induced cardiomyocyte hypertrophy. **A**. Table shows the details of selected genes that are used for validation and experimentation. Relative transcript abundance from each sample is shown, along with shrunken Log2FC and adjusted p-value (padj). The table also lists the Gene ID, chromosomal location and length. **B**. Relative transcript abundance of selected genes as measured by quantitative polymerase chain reaction (qPCR) in neonatal rat ventricular cardiomyocytes (NRVM) treated with ad-siG3bp1 or ad-siLUC in the absence or presence of ET-1. Error bars represents SEM, * is $p<0.05$ compared to siLUC (control), # is $p<0.05$ compared to siLUC+ET-1. **C**. Western

blotting with protein lysates from NRVM treated with ad-siLUC or increasing doses of ad-siG3bp1 with or without ET-1 stimulation. The membrane was probed for the indicated antibodies. Gapdh and LaminA/C are shown as loading controls. Anti-Myosin (slow, skeletal) recognizes cardiac βMHC. Protein ladders in KDa. **D**. Immunocytochemisty on NRVM plated on glass slides coated with 0.3% gelatin, treated with ad- siLUC or increasing doses of ad-siG3bp1 with or without ET-1 (100nM) for 20hrs, fixed and probed with anti-G3bp1, anti-a-actinin and DAPI, colors as indicated. All experiments were repeated at least in three independent cultures (n=3). **E** and **F**. Immunocytochemisty and cardiomyocyte surface area (image J), respectively on NRVM plated on glass slides coated with 0.3% gelatin, treated with ad-siLUC or increasing doses of ad-siG3bp1 stimulated with PE (100μM) for 18–20hrs, fixed and probed with anti-α-actinin, as indicated (n=2).

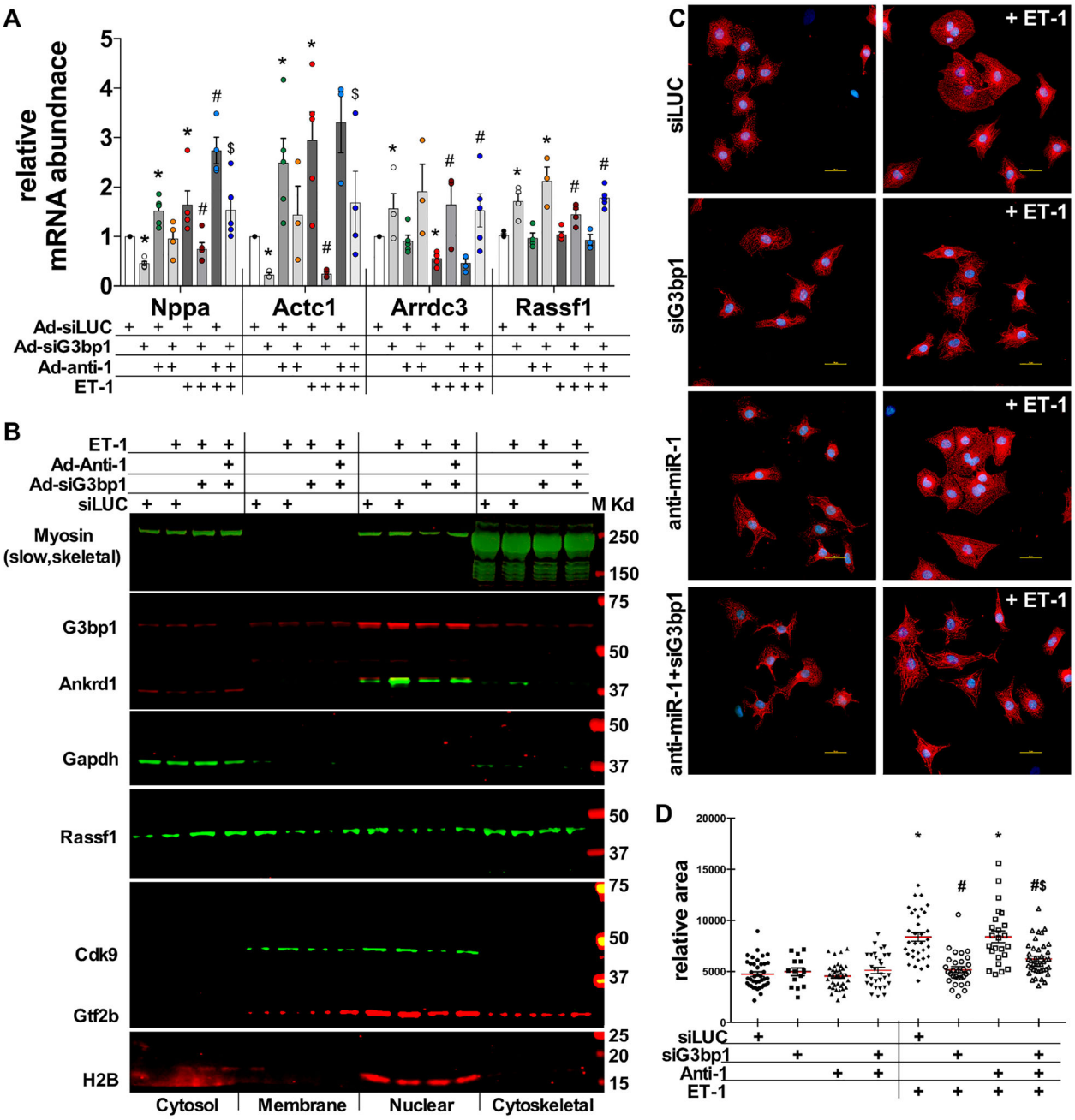

Figure 3.

G3bp1-miR-1 axis regulates cardiomyocyte hypertrophy. **A**. Graph represents relative transcript abundance as measured by qPCR of selected genes treated with siLUC, siG3bp1 and/or anti-miR-1 (as indicated) with or without ET-1 stimulation in NRVM. Error bars represents SEM, * is $p<0.05$ compared to siLUC, # is $p<0.05$ compared to ET-1 and $ is $p<0.05$ compared to siG3bp1+ET-1. **B**. Western blot on fractionated protein lysates from NRVM treated with siLUC, siG3bp1 and/or anti-miR-1 with or without ET-1 stimulation. The membranes were stripped and probed for indicated specific antibodies. Gapdh, H2b and Myosin are shown as specificity controls of cytoplasm, nuclear and cytoskeletal fractions.

Gapdh and H2b also serve as loading controls. Cdk9 and Gtf2b were shown as validated targets of miR-1 in cardiomyocytes. **C**. Immunocytochemisty on NRVM plated on glass slides coated with 0.3% gelatin, treated with ad- siLUC or ad-siG3bp1 with or without ET-1 (100nM) for 20hrs, fixed and probed with anti-α-actinin and DAPI. **D**. Cell surface area of NRVM treated as indicated in C, is measured using Image J, plotted and shown in graph as relative area. Error bars are SEM, * is $p<0.05$ compared to siLUC, # is $p<0.05$ compared to ET-1 and $ is $p<0.05$ compared to siG3bp1+ET-1. All experiments were repeated at least in three independent cultures (n=3).

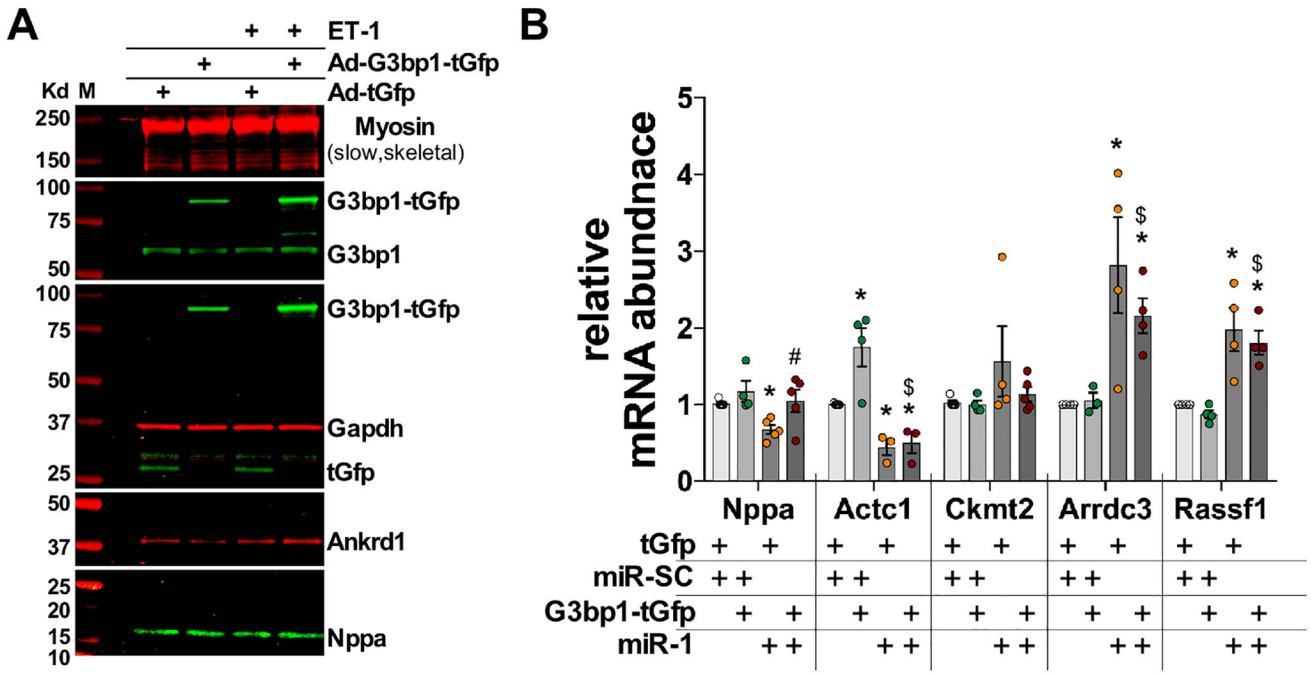

Figure 4.

Exogenous G3bp1 rescues miR-1 induced change in gene expression. **A**. Western blot with lysates from NRVM treated with ad-tGfp or ad-G3bp1-tGfp with or without ET-1 stimulation. The blots were probed for the indicated antibodies. Gapdh is shown as internal loading control. **B**. Graph represents relative mRNA abundance as measured by qPCR of selected genes treated with ad-tGfp, ad-G3bp1-tGfp and/or ad-miR-1. Error bars represents SEM, * is $p<0.05$ compared to tGfp, # is $p<0.05$ compared to miR-1 and $ is $p<0.05$ compared to G3bp1-tGfp. n=3–4 independent cardiomyocyte cultures.

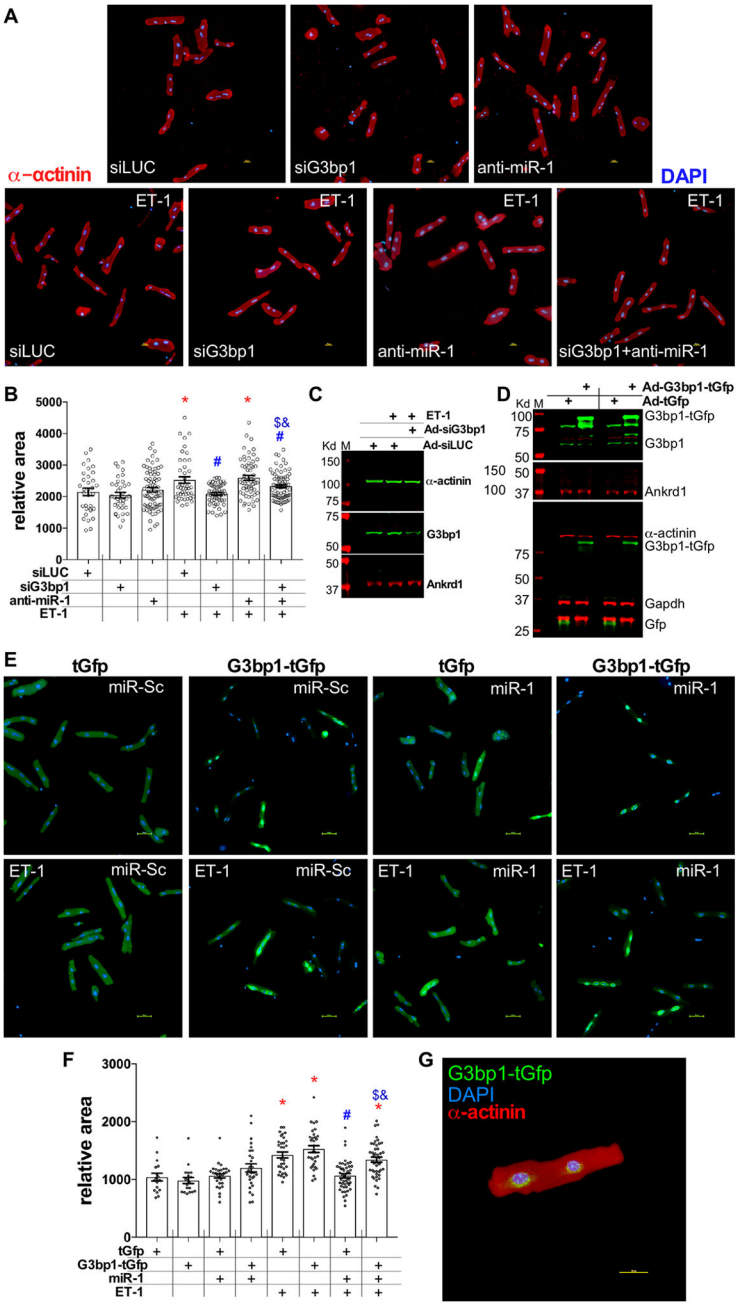

Figure 5.

G3bp1–miR-1 signaling in adult cardiomyocytes. **A**. Immunocytochemistry on isolated adult mouse ventricular myocytes (AMVM) treated with ad-siLUC, ad-siG3bp1 and/or ad-anti-miR-1 with or without ET-1. Cells were fixed and stained for a-actinin and DAPI. **B**. Graph represents the relative area of AMVM treated as indicated in A. Error bars represents SEM, * is p<0.05 compared to siLUC, # is p<0.05 compared to siLUC+ET-1, $ is p<0.05 compared to siG3bp1+ET-1 and & is p<0.05 compared to anti-miR-1+ET-1. **C**. Western blots on lysates from AMVMs treated with ad-siLUC or ad-siG3bp1 with or without ET-1. The blots were probed for the indicated antibodies. **D**. Western blotting on

lysates from AMVMs treated with ad-tGfp or ad-G3bp1-tGfp. The blots were probed for the indicated antibodies. **E**. Immunocytochemistry on isolated adult mouse ventricular myocytes (AMVM) treated with ad-tGfp, ad-G3bp1-tGfp and/or ad-miR-1 with or without ET-1. Cells were fixed, mounted and visualized for Gfp signal. **F**. Graph represents the relative area of AMVM treated as indicated in E. Error bars represents SEM, * is $p<0.05$ compared to tGfp, # is $p<0.05$ compared to tGfp+ET-1, $ is $p<0.05$ compared to G3bp1-tGfp+ET-1 and & is $p<0.05$ compared to miR-1+ET-1. **G**. Image of adult mouse ventricular myocytes at 60X magnification showing Gfp localization with respect to a-actinin (cardiomyocyte structure) and DAPI (nucleus). All experiments were performed in triplicates from three independent cultures, unless indicated.